Observations of Sharp Oxalate Reductions in Stratocumulus Clouds at Variable Altitudes: Organic Acid and Metal Measurements During the 2011 E-PEACE Campaign

Armin Sorooshian[1,2*], Zhen Wang[1], Matthew M. Coggon[3], Haflidi H. Jonsson[4], Barbara Ervens[5,6]

1. Chemical and Environmental Engineering, University of Arizona, Tucson, AZ, United States.
2. Atmospheric Sciences, University of Arizona, Tucson, AZ, United States.
3. Department of Chemical Engineering, California Institute of Technology, Pasadena, CA, United States.
4. Center for Interdisciplinary Remotely Piloted Aircraft Studies, Naval Postgraduate School, Monterey, CA, United States.
5. Cooperative Institute for Research in Environmental Sciences, University of Colorado, Boulder, CO, United States.
6. Chemical Sciences Division, NOAA Earth System Research Laboratory, Boulder, CO, United States.

Supporting Information Summary: 6 Pages including Cover Page, 2 Figures, 2 Tables, and references

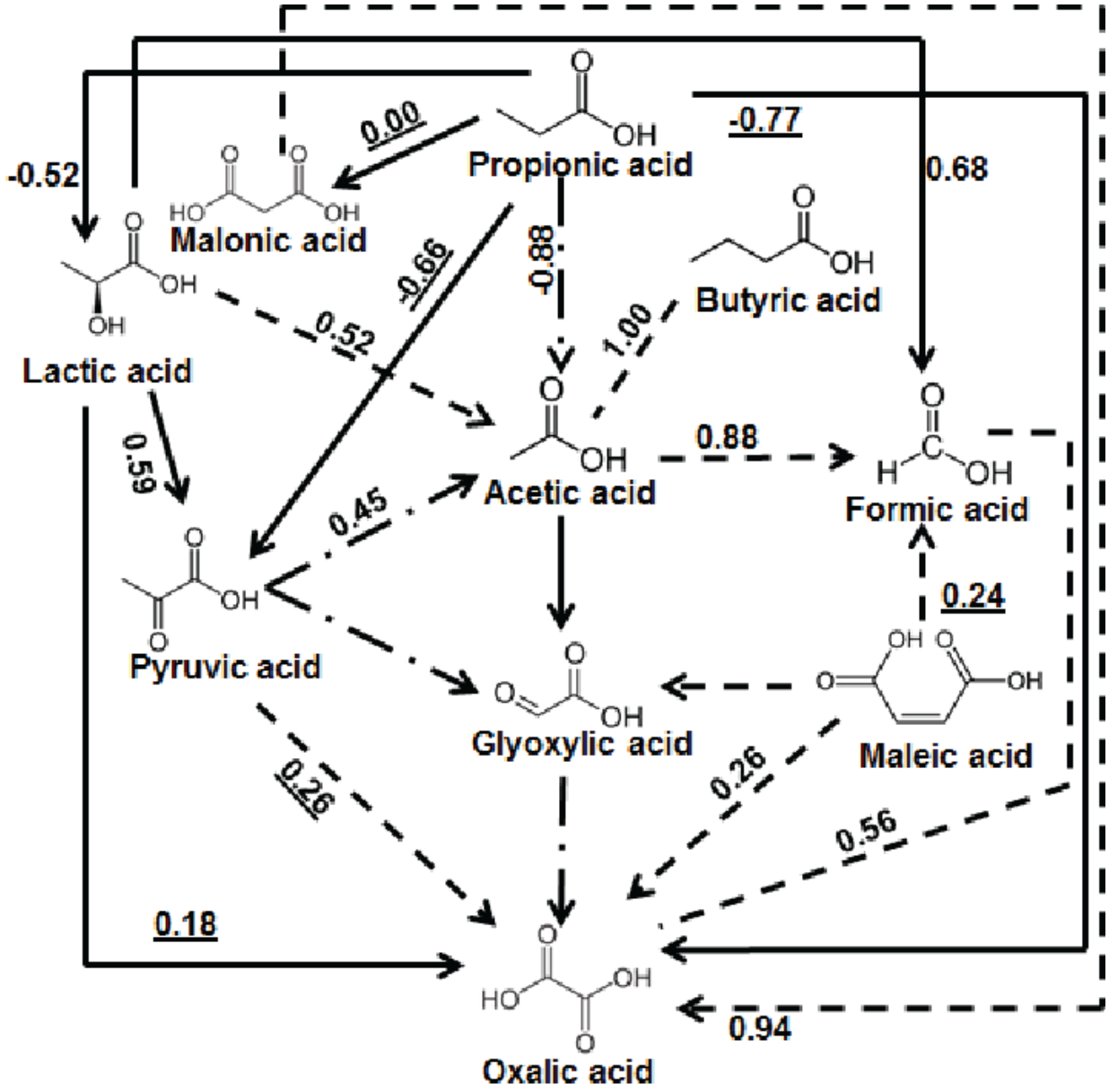

Figure S1. A visual schematic of relationships between organic acids in cloud water. The solid lines with arrows represent documented pathways and dashed lines with arrows represent a documented pathway with intermediate steps in between (*1-8*). Dashed lines with no arrows lack a documented reaction pathway to our knowledge. Numbers signify statistically-significant correlation coefficients (r) at 95% confidence using a student's two-tailed t-test; underlined correlation coefficients are statistically insignificant. Glyoxylate could not be quantified, but only detected in seven samples; six of those samples had oxalate detected, five had pyruvate, three had acetate, and six had maleate.

1. Box model description

1.1 Chemical mechanism

The chemical mechanism in the box model includes the oxidation of anthropogenic and biogenic precursors that lead to the formation of water-soluble compounds that are taken up into the aqueous phase and are oxidized there to form organic acids. The mechanism has been used previously to explore the production of di- and ketocarboxylic acids in clouds [Tables 1-3 in (*3*)]. In the current study we have extended the aqueous-phase mechanism by the redox-cycling of iron with the processes summarized in Table S1. All rate constants are taken from the 'Chemical aqueous-phase radical mechanism' (CAPRAM, version 2.4 (MODAC mechanism); (*9)* and http://projects.tropos.de/capram/).

Table S1. Summary of iron reactions and equilibria considered in the model simulations.

Irreversible reactions			
	Rate constant		
$Fe^{2+} + H_2O_2 \rightarrow OH + OH^- + Fe^{3+}$	$50\ M^{-1}\ s^{-1}$		
$O_2^- + Fe^{3+} \rightarrow H_2O_2 + Fe^{3+}$	$1.5\cdot10^8\ M^{-1}\ s^{-1}$		
$O_2^- + [Fe(OH)]^{2+} \rightarrow H_2O_2 + Fe^{3+} + OH^-$	$1.5\cdot10^8\ M^{-1}\ s^{-1}$		
$O_2^- + [Fe(OH)_2]^{+} \rightarrow H_2O_2 + Fe^{3+} + 2\ OH^-$	$1.5\cdot10^8\ M^{-1}\ s^{-1}$		
$HO_2 + [Fe(OH)]^{2+} \rightarrow H_2O_2 + Fe^{3+} + OH^-$	$1.3\cdot10^5\ M^{-1}\ s^{-1}$		
$OH + Fe^{2+} \rightarrow [Fe(OH)]^{2+}$			
Photolysis processes[1)]			
$[Fe(OH)]^{2+} + h\nu \rightarrow Fe^{2+} + OH$	$4.51\cdot10^{-3}\ s^{-1}$	$\Phi = 0.312$	
$[Fe(OH)_2]^{+} + h\nu \rightarrow Fe^{2+} + OH + OH^-$	$5.77\cdot10^{-3}\ s^{-1}$	$\Phi = 0.255$	
$[Fe(C_2O_4)_2]^- + h\nu \rightarrow Fe^{2+} + C_2O_4^{2-} + CO_2 + O_2^-$	$2.47\cdot10^{-2}\ s^{-1}$	$\Phi = 1$	
$[Fe(C_2O_4)_3]^{3-} + h\nu \rightarrow Fe^{2+} + 2\ C_2O_4^{2-} + CO_2 + O_2^-$	$1.55\cdot10^{-2}\ s^{-1}$	$\Phi = 0.6$	
Equilibria			
	K	k(forward)	k(back)
$H_2C_2O_4 \rightleftharpoons HC_2O_4^- + H^+$	$6.4\cdot10^{-2}$	$3.2\cdot10^9$	$5\cdot10^{10}$
$HC_2O_4^- \rightleftharpoons C_2O_4^{2-} + H^+$	$5.25\cdot10^{-5}$	$2.6\cdot10^6$	$5\cdot10^{10}$
$Fe^{3+} + H_2O \rightleftharpoons [Fe(OH)]^{2+} + H^+$	$1.1\cdot10^{-4}$	$4.7\cdot10^4\ M^{-1}\ s^{-1}$	$4.3\cdot10^8\ M^{-1}\ s^{-1}$
$[Fe(OH)]^{2+} + H_2O \rightleftharpoons [Fe(OH)_2]^{+} + H^+$	$1.4\cdot10^{-7}$	$1.1\cdot10^3\ M^{-1}\ s^{-1}$	$8\cdot10^9\ M^{-1}\ s^{-1}$
$Fe^{3+} + C_2O_4^{2-} \rightleftharpoons [Fe(C_2O_4)]^+$	$2.9\cdot10^9\ M$	$8.7\cdot10^6\ M^{-1}\ s^{-1}$	$3\cdot10^{-3}\ s^{-1}$
$[Fe(C_2O_4)]^+ + C_2O_4^{2-} \rightleftharpoons [Fe(C_2O_4)_2]^-$	$6.3\cdot10^6\ M$	$1.89\cdot10^4\ M^{-1}\ s^{-1}$	$3\cdot10^{-3}\ s^{-1}$
$[Fe(C_2O_4)_2]^{2-} + C_2O_4^{2-} \rightleftharpoons [Fe(C_2O_4)_3]^{3-}$	$3.8\cdot10^4\ M$	$114\ M^{-1}\ s^{-1}$	$3\cdot10^{-3}\ s^{-1}$

[1)] reported photolysis rates are the maximum values; in the model they are adjusted as a function of location and time of day using the quantum yields Φ

1.2. Initial conditions

The initial conditions are similar to the 'clean scenario' in (*3*). However, in order to take into account higher emissions due to the ship plumes, we increased SO_2, VOCs, and NO_x. All initial mixing ratios are summarized in Table S2. For the different simulations, we assume different fractions of iron [0, 1, 2, 3, and 4.5 ng m^{-3}] in the initial aerosol mass (~ 5 μg m^{-3}) that are dissolved in the cloud droplets.

Table S2. Initial mixing ratios in model simulations.

Species	ppb
SO_2	1.5
O_3	30
H_2O_2	1
NH_3	0.1
HNO_3	0.1
CO_2	360,000
N_2O_5	0.02
HCHO	1
Hydroxyacetone	0.1
Glyoxal	1
Methylgyoxal	1
Formic acid	0.1
Acetic acid	0.1
NO_x	10
Toluene	5
Ethylene	2
Cyclohexene	0.1
Isoprene	2

1.3. Model simulations

1.3.1 Model set up

The model does not include any microphysical processes that describe droplet activation/evaporation. Instead, simulations are performed for continuous air/droplet interaction. The simulation time of three hours corresponds to an estimate for the total time particles might be processed in clouds during their trajectory along the coast in the study region (Figure 3). This estimate is based on the assumption that an individual droplet in stratocumulus clouds lives on the order of a few minutes (~ 5 – 20 min / hour; (*9*)) and each particle is cycled several times through clouds. The total liquid water content (LWC = 0.3 g m^{-3}) is chosen as an average value of the observed ones (Table 3). This LWC is distributed to five drop classes with ~8 μm < D_{drop} < ~30 μm that have been fitted to observed drop distributions. In agreement with size-resolved measurements in radiation fogs, we assumed that both iron and H^+ concentrations decrease with increasing drop size (*10*). Specifically, we assumed an increase from pH = 3.3 to 3.7 that resulted in an average pH = 3.52 in agreement with values as determined in the cloud water samples. Iron

concentrations ranged from ~ 0.8 μM to ~ 0.06 μM from the small to large droplets (in the case of the highest assumed Fe mass, 8.3 ng m^{-3}).

While LWC and droplet size might affect the total predicted oxalate concentration, it is assumed that they affect it to similar extents in the simulations with and without iron, respectively, and thus a comparison of the results is meaningful in this simplified setup.

1.3.2 Model results

Figure S2 shows predicted size-resolved oxalate mass concentrations based on the simulations as discussed in Section 3.3 of the main manuscript.

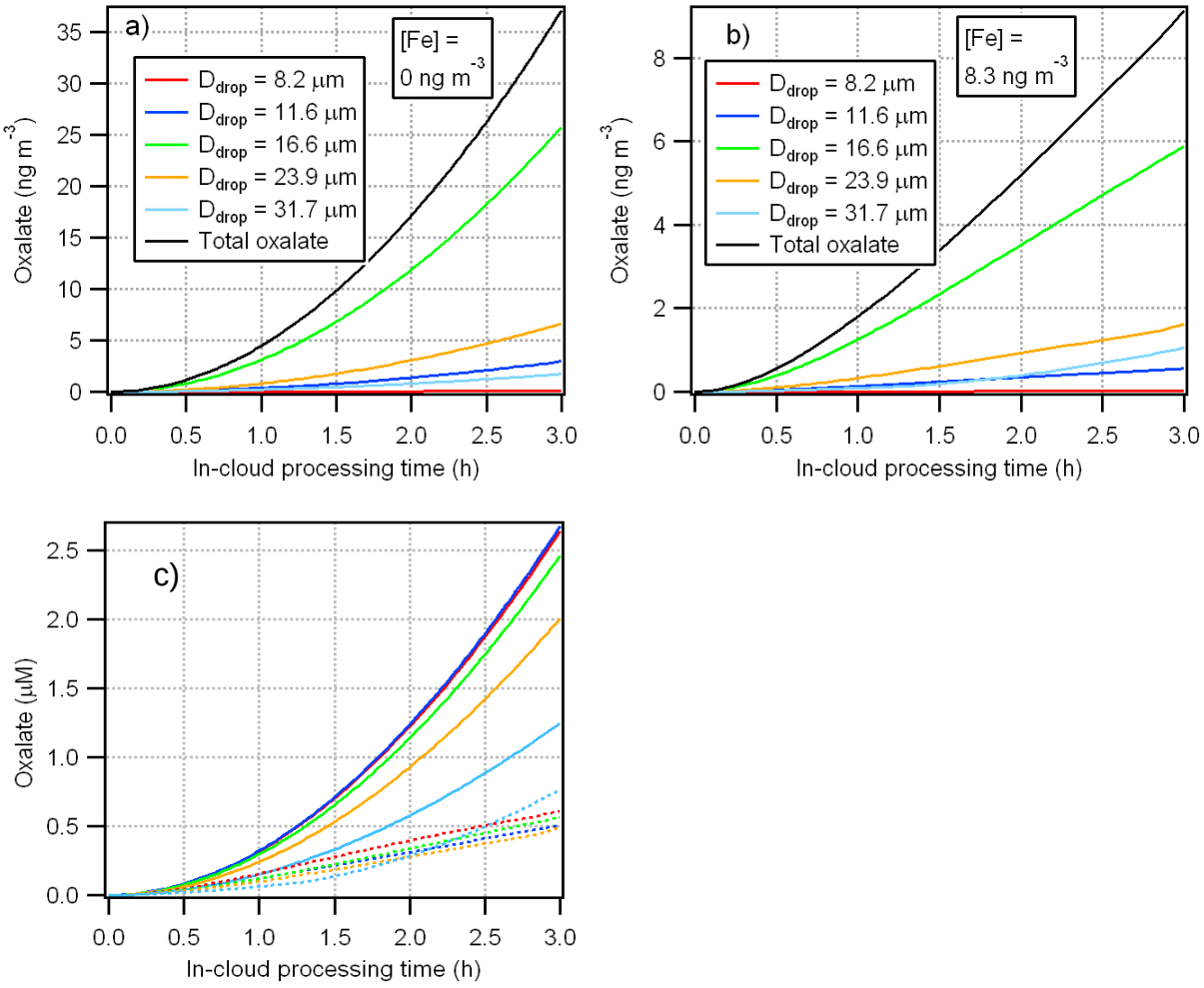

Figure S2. Predicted oxalate concentration as a function of drop diameter a) without iron; b) Fe = 8.3 ng m^{-3}; c) predicted aqueous-phase concentrations of oxalate (dotted lines: Fe = 8.3 ng m^{-3}; solid lines: without iron).

References

(1) Carlton, A. G.; Turpin, B. J.; Lim, H. J.; Altieri, K. E.; Seitzinger, S. Link between isoprene and secondary organic aerosol (SOA): Pyruvic acid oxidation yields low volatility organic acids in clouds. *Geophys. Res. Lett*. **2006**, *33*, L06822, doi:10.1029/2005GL025374.

(2) Charbouillot, T.; Gorini, S.; Voyard, G.; Parazols, M.; Brigante, M.; Deguillaume, L.; Delort, A. M.; Mailhot, G. Mechanism of carboxylic acid photooxidation in atmospheric aqueous phase: Formation, fate and reactivity. *Atmos. Environ*. **2012**, *56*, 1-8.

(3) Ervens, B.; Feingold, G.; Frost, G. J.; Kreidenweis, S. M. A modeling study of aqueous production of dicarboxylic acids: 1. Chemical pathways and speciated organic mass production, *J. Geophys. Res.* **2004**, *109*, D15205,doi:10.1029/2003JD004387.

(3) Gallimore P. J.; Achakulwisut, P.; Pope, F. D.; Davies, J. F.; Spring, D. R.; Kalberer, M. Importance of relative humidity in the oxidative ageing of organic aerosols: case study of the ozonolysis of maleic acid aerosol. *Atmos. Chem. Phys*. **2011**, *11*, 12181–12195.

(4) Liu, Y., Monod, A., Tritscher, T., Praplan, A. P., DeCarlo, P. F., Temime-Roussel, B., Quivet, E., Marchand, N., Dommen, J., Baltensperger, U. Aqueous phase processing of secondary organic aerosol from isoprene photooxidation, *Atmos. Chem. Phys.* **2012**, *12*, 5879-5895, doi:10.5194/acp-12-5879-2012.

(5) Nájera, J. J.; Percival, C. J.; Horn, A. B. Kinetic studies of the heterogeneous oxidation of maleic and fumaric acid aerosols by ozone under conditions of high relative humidity. *Phys. Chem. Chem. Phys*. **2010**, *12*, 11417–11427.

(6) Stefan, M.I., Hoy, A.R., Bolton, J.R.. Kinetics and mechanism of the degradation and mineralization of acetone in dilute aqueous solution sensitized by the UV photolysis of hydrogen peroxide. *Environ. Sci. Technol.* **1996**, *30*, 2382–2390.

(7) Stefan, M. I.; Bolton, J. R. Reinvestigation of the acetone degradation mechanism in dilute aqueous solution by the UV/ H2O2 process. *Environ. Sci. Technol.* **1999**, *33*, 870-873.

(8) Warneck, P. In-cloud chemistry opens pathway to the formation of oxalic acid in the marine atmosphere. *Atmos. Environ.* **2003**, *37*, 2423-2427.

(9) Feingold, G.; Kreidenweis, S. M.; Zhang, Y. P. Stratocumulus processing of gases and cloud condensation nuclei - 1. Trajectory ensemble model. *J. Geophys. Res.* **1998,** *103*, (D16), 19527-19542.

(10) Rao, X.; Collett, J. L. The drop size-dependence of iron and manganese in clouds and fogs: implications for sulfate production. *J. Atmos. Chem.* **1998**, *30*, 273-289.